

High Efficiency Transformerless Interleaved Step- Down Conversion Ratio Dc-Dc Converter

Ms.K.Sudha.,B.E.,
PG Scholar department of Power Electronics And Drives
AVS Engineering College,
Ammamet, Salem,
Tamilnadu.
jencysudha94@gmail.com

ABSTRACT:

This project presents, a novel transformerless interleaved high step-down conversion ratio dc-dc converter with low switch voltage stress. In the proposed converter, two input capacitors are series-charged by the input voltage and parallel discharged by a new two-phase interleaved buck converter for providing a much higher step-down conversion ratio without adopting an extreme short duty cycle. Based on the capacitive voltage division, the main objectives of the new voltage-divider circuit in the converter are for both storing energy in the blocking capacitors for increasing the step-down conversion ratio and reducing voltage stresses of active switches. The proposed converter topology possesses the low switch voltage stress characteristic. This will allow one to choose lower voltage rating MOSFETs to reduce both switching and conduction losses, and the overall efficiency is consequently improved.

Keywords: MOSFET-Metal Oxide Semiconductor Field Effect Transistor.

I.INTRODUCTION

A DC-to-DC converter is an electronic circuits which converts a source of direct current (DC) from one voltage level to another. It is a class of power converter. DC-DC power converters are employed in a variety of applications, including power supplies for personal computers, office equipment, spacecraft power systems, laptop computers, and telecommunications equipment, as well as dc motor drives. The input to a dc-dc converter is an unregulated dc voltage V_g . The converter produces a regulated output voltage V , having a magnitude that differs from V_g . Such electronic devices often contain several sub-circuits, each with its own voltage level requirement different from that supplied by the battery or an

external supply (sometimes higher or lower than the supply voltage). Additionally, the battery voltage declines as its stored energy is drained. Switched DC to DC converters offer a method to increase voltage from a partially lowered battery voltage thereby saving space instead of using multiple batteries to accomplish the same thing.

Step down transformers are a standard type of single phase distribution transformers, with primary voltages of 120, 240 or 480 volts and secondaries typically of 12, 16, 24, 32 or 48 volts. They are available in sizes ranging from 50 volt amperes to 10 kilo-volt amperes. Thus the universal range AC supply is step down to our required AC voltage range.

This change of technology may bring several advantages:

INTERLEAVED BUCK CONVERETER:

Interleaving technique is used in some applications due to its advantages regarding filter reduction, dynamic response, and power management. Using interleaving, the power stage of a converter is divided into several and smaller power stages. Therefore, the size of each component is reduced. With a very high number of interleaved phases, the current stress is greatly reduced and using a different technology becomes a possibility.

- power converter is made of surface mount technology(SMT) components;
- automatic assembly;
- absence of heat sinks (usually heat sinks require manual assembly);
- magnetic components can be planar or SMT. Repetitively is greatly increased;
- very small input and output filters

II. CONVENTIONAL SYSTEM

A. INTRODUCTION

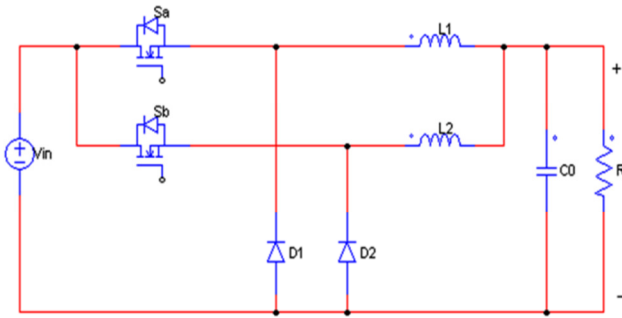


Figure.2.1 Configuration of conventional IBC

The conventional circuit consists of two active power switches, two diodes and two inductors. Conventional IBC shown in Fig.2.1, because active switch devices suffer from the input voltage, high voltage devices rated above the input voltage should be applied. High-voltage-rated devices are generally with poor characteristics such as high cost, large ON-resistance, large voltage drop, severe reverse recovery, etc.

B. DRAWBACK OF EXISTING SYSTEM:

The above parameters limit the switching frequency of the converter and impact the power density improvement. For high-input and low-output voltage regulation applications, pursuing higher power density and better dynamics, it is required operating at higher switching frequencies that will increase both switching and conduction losses. Consequently, the efficiency is further deteriorated. Also, it experiences an extremely short duty cycle in the case of high input and low-output voltage applications.

III. PROPOSED SYSTEM

A. INTRODUCTION

Recently, high-performance dc-dc converters have been called for the increasing high step-down ratios with high output current rating applications, such as VRMs of CPU boards and battery chargers, and distributed power systems. For nonisolation applications with low output current ripple requirement, an interleaved buck converter (IBC) has received a lot of attention due to its simple structure and low control complexity.

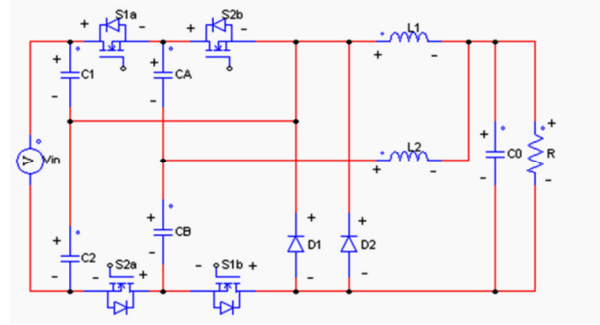


Figure 3.1.configuration of proposed converter

To overcome the drawbacks of the conventional IBC, many step-down converters have been proposed. A quadratic buck converter is synthesized by cascading two dc-dc buck converters which have the voltage conversion ratios of two cascaded converters but with fewer switches. It can operate with wider ranges of step-down conversion ratio than those of conventional single-switch converters without an extremely short duty ratio. However, it operates two cascaded converters and thus processes energy so that the efficiency is worse. A three-level buck converter is proposed to reduce the switch voltage stress to half of the input voltage. By using the aforementioned converter, low-voltage MOSFETs have higher efficiency and better performance compared with the conventional buck converter. However, so many components are required for the use of IBC.

B. OPERATING PRINCIPLE

The proposed novel transformerless IBC is shown in Fig. 3.1. From Fig. 3.1, the proposed converter consists of two inductors, four active power switches, two diodes, and four capacitors.

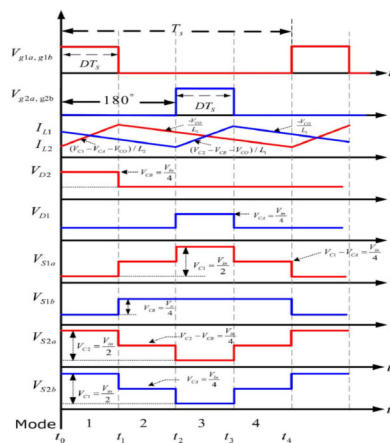


Figure 3.2.Key waveforms of the proposed converter at CCM

The main objectives of the four capacitors are twofold. First, they are used to store energy as usual. Second, based on the capacitive voltage division principle, they are used to reduce the voltage stress of active switches as well as to increase the step-down conversion ratio. Basically, the operating principle of the proposed converter can be classified into four operation modes. The interleaved gating signals with an 180° phase shift as well as some key operating waveforms are shown in Fig. 3.3. As the main objective is to obtain a high step-down conversion ratio and as such characteristic can only be achieved when the duty cycle is less than 0.5 and in CCM, hence the steady-state analysis is made only for this case. However, in DCM, as there is not enough energy transfer from the blocking capacitors to the inductors, output capacitors, and load side, and as, consequently, it is not possible to get the charge balance of the blocking capacitor, then the nice automatic uniform current sharing property will be lost, and additional current-sharing control between phases should be included under this condition.

C. MODES OF OPERATION

1) Mode 1 [$t_0 < t \leq t_1$]:

During this mode, S1a, S1b, and D1 are turned on, while S2a, S2b, and D2 are turned off. The corresponding equivalent circuit is shown in Fig. 3.4(a). From Fig. 3.4(a), one can see that, during this mode, current i_{L1} freewheels through D1, and L1 is releasing energy to the output load. However, current i_{L2} provides two separate current paths through CA and CB. The first path starts from C1, through S1a, CA, L2, CO and R, and D1 and then back to C1 again. Hence, the stored energy of C1 is discharged to CA, L2, and output load. The second path starts from CB, through L2, CO and R, and S1b and then back to CB again. In other words, the stored energy of CB is discharged to L2 and output load. Therefore, during this mode, i_{L2} is increasing, and i_{L1} is decreasing, as can be seen from Fig. 3.3. Also, from Fig. 4(a), one can see that V_{C1} is equal to V_{CA} plus V_{CB} due to conduction of S1a, S1b, and D1. Since $V_{C1} = V_{in}/2$ and $V_{CA} = V_{CB} = V_{C1}/2 = V_{in}/4$,

one can observe from Fig. 3.4(a) that the voltage stress of D2 is equal to $V_{CB} = V_{in}/4$ and the voltage stresses of S2a and S2b are clamped to $V_{C2} = V_{in}/2$ and $V_{C1} = V_{in}/2$, respectively.

The corresponding state equations are given as follows:

$$L_1 \frac{di_{L1}}{dt} = -V_{CO} \quad (3.1)$$

$$L_2 \frac{di_{L2}}{dt} = V_{C1} - V_{CA} - V_{CO} \\ = V_{CB} - V_{CO} \quad (3.2)$$

$$(C_1 + C_2) \frac{dv_{C1}}{dt} = -i_{CA} \quad (3.3)$$

$$C_A \frac{dv_{CA}}{dt} = i_{L2} + i_{CB} \quad (3.4)$$

$$C_B \frac{dv_{CB}}{dt} = i_{CA} - i_{L2} \quad (3.5)$$

$$C_0 \frac{dv_{CO}}{dt} = i_{L1} + i_{L2} - \frac{v_{CO}}{R} \quad (3.6)$$

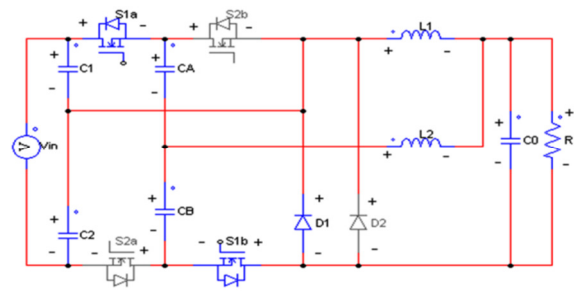


Figure 3.3(a). Equivalent circuit for the proposed converter for Mode 1

2) Mode 2 [$t_1 < t \leq t_2$]:

During this mode, S1a, S1b, S2a, and S2b are turned off. The corresponding equivalent circuit is shown in Fig. 3.4(b). From Fig. 3.4(b), one can see that both i_{L1} and i_{L2} are freewheeling through D1 and D2, respectively. Both V_{L1} and V_{L2} are equal to $-V_{CO}$, and hence, i_{L1} and i_{L2} decrease linearly. During this mode, the voltage across S1a, namely, V_{S1a} , is equal to the difference of V_{C1} and V_{CA} ,

And V_{S1b} is clamped at V_{CB} . Similarly, the voltage across S2a, namely, V_{S2a} , is equal to the difference of V_{C2} and V_{CB} , and V_{S2b} is clamped at V_{CA} . The corresponding state equations are given as follows:

$$L_1 \frac{di_{L1}}{dt} = -V_{CO} \quad (3.7)$$

$$L_2 \frac{di_{L2}}{dt} = -V_{CO} \quad (3.8)$$

$$(C_1 + C_2) \frac{dv_{C1}}{dt} = 0 \quad (3.9)$$

$$C_A \frac{dv_{CA}}{dt} = 0 \quad (3.10)$$

$$C_B \frac{dv_{CB}}{dt} = 0 \quad (3.11)$$

$$C_0 \frac{dv_{C0}}{dt} = i_{L1} + i_{L2} - \frac{v_{C0}}{R} \quad (3.12)$$

$$L_2 \frac{di_{L2}}{dt} = -V_{C0} \quad (3.14)$$

$$(C_1 + C_2) \frac{dv_{C1}}{dt} = -i_{CB} \quad (3.15)$$

$$C_A \frac{dv_{CA}}{dt} = i_{CB} - i_{L1} \quad (3.16)$$

$$C_B \frac{dv_{CB}}{dt} = i_{CA} + i_{L1} \quad (3.17)$$

$$C_0 \frac{dv_{C0}}{dt} = i_{L1} + i_{L2} - \frac{v_{C0}}{R} \quad (3.18)$$

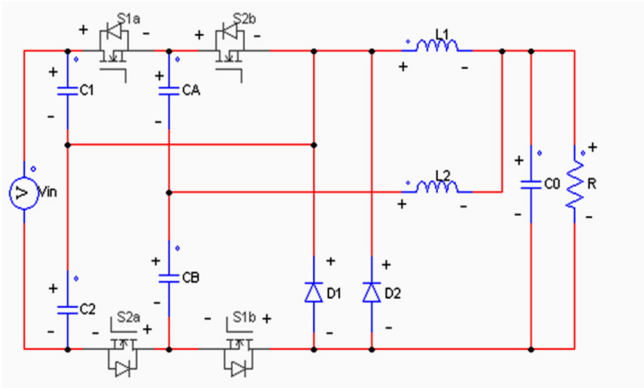


Figure 3.3(b). Equivalent circuit for the proposed converter for Mode 2

3) Mode 3 [$t_2 < t \leq t_3$]:

During this mode, S2a, S2b, and D2 are turned on, while S1a, S1b, and D1 are turned off. The corresponding equivalent circuit is shown in Fig. 3.4(c). From Fig. 3.4(c), one can see that, during this mode, current i_{L2} is freewheeling through D2, and L2 is releasing energy to the output load. However, current i_{L1} provides two separate current paths through CA and CB. The first path starts from C2, through L1, C0 and R, D2, CB, and S2a and then back to C2 again. Hence, the stored energy of C2 is discharged to CB, L1, and output load. The second path starts from CA, through S2b, L1, C0 and R, and D2 and then back to CA again. In other words, the stored energy of CA is discharged to L1 and output load. Therefore, during this mode, i_{L1} is increasing, and i_{L2} is decreasing, as can be seen from Fig. 3.3. Also, from Fig. 3.4(c), one can see that V_{C2} is equal to V_{CA} plus V_{CB} due to conduction of S2a and S2b. Since $V_{C2} = V_{in}/2$ and $V_{CA} = V_{CB} = V_{C2}/2 = V_{in}/4$, one can observe from Fig. 3.4(c) that the voltage stress of D1 is equal to $V_{CA} = V_{in}/4$ and the voltage stresses of S1a and S1b are clamped to $V_{C1} = V_{in}/2$ and $V_{CB} = V_{in}/4$, respectively. The corresponding state equations are given as follows:

$$L_1 \frac{di_{L1}}{dt} = V_{in} - V_{C1} - V_{CB} - V_{C0} \quad (3.13)$$

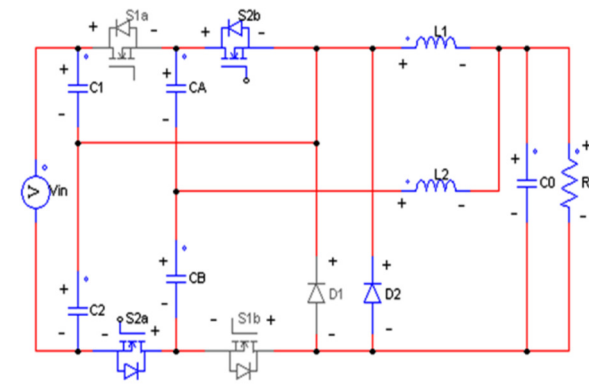


Figure 3.3(c). Equivalent circuit for the proposed converter for Mode 3

4) Mode 4 [$t_3 < t \leq t_4$]:

For this operation mode, as can be observed from Fig. 3, S1a, S1b, S2a, and S2b are turned off. The corresponding equivalent circuit turns out to be the same as Fig. 3.4(b), and its operation is the same as that of mode 2. From the aforementioned illustration of the proposed converter, one can see that not only the control is very simple but also the operations of two phases are both symmetric and rather easy to understand. Also, from the key operating waveforms of the proposed converter shown in Fig. 3.3, one can see clearly the low voltage stress characteristic of four active switches and two diodes as well as the uniform current sharing.

D. STEADY-STATE ANALYSIS

In order to simplify the circuit analysis of the proposed converter, some assumptions are made as follows.

- 1) All components are ideal components.
- 2) The capacitors are sufficiently large such that the voltages across them can be considered constant. Also, assume that $C_1 = C_2$ and $CA = CB$.

3) The system is under steady state and is operating in CCM with duty ratio being lower than 0.5 for high step-down conversion ratio purposes.

E. CONTROL STRATEGIES

In all cases, it is shown that the average value of the output voltage can be varied. The two types of control strategies (schemes) are employed in all cases. These are: (1) Time-ratio control, and (2) Current limit control

1) TIME-RATIO CONTROL

In the time ratio control the value of the duty ratio, $K = T_{ON}/T$ is varied. There are two ways, which are constant frequency operation, and variable frequency operation.

2) CONSTANT FREQUENCY OPERATION

In this control strategy, the ON time, is varied, keeping the frequency ($F=1/T$), or time period T constant. This is also called as pulse width modulation control (PWM). Two cases with duty ratios, as (a) 0.25 (25%), and (b) 0.75 (75%) are shown in Fig.4.6. Hence, the output voltage can be varied by varying ON time.

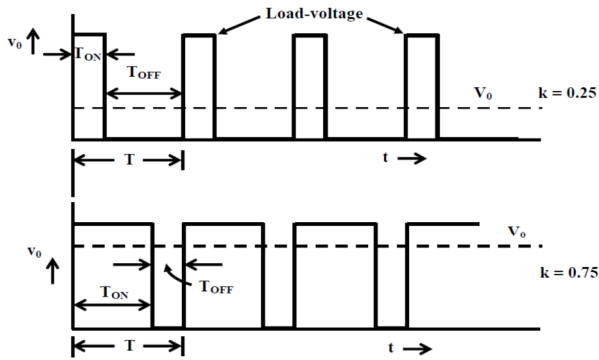


Figure 4.7 Pulse-width modulation control (constant frequency)

IV. SIMULATION OF PROPOSED CONVERTER

The performance of the proposed circuit is verified by the prototype. The IBCs are operated when the duty cycle is less than 0.5. The components are chosen and values are given in Table II.

The specifications of the proposed converter are the following:

i) input voltage of 400 VDC

ii) output voltage of 25 VDC

iii) power rating of 400 W

iv) switching frequency of 40 kHz.

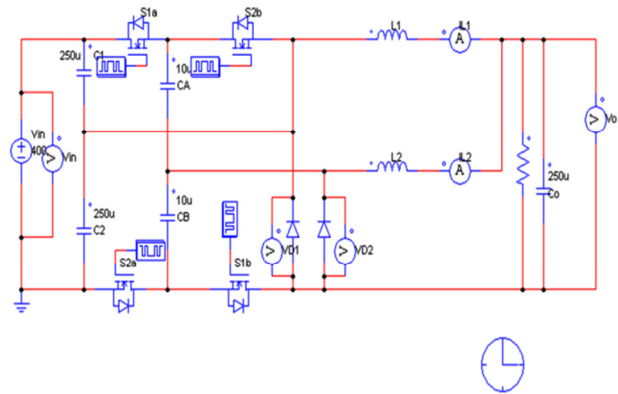


Figure.4.1 Simulation diagram of transformerless interleaved buck converter

TABLE II
COMPONENT PARAMETERS OF THE PROTOTYPE SYSTEM

Components	Specification
Inductors (L_1, L_2)	CM467060, 250 μ H
Active Switches ($S_{1a}, S_{1b}, S_{2a}, S_{2b}$)	IXFH100N25P, 250V, $R_{ds(on)}=27m\Omega$
Active Switch S_{D1}	IXFH150N15P, 150V, $R_{ds(on)}=13m\Omega$
Blocking capacitors (C_A, C_B)	10 μ F/250V ($R_s=4.6m\Omega$)
Input capacitors (C_1, C_2)	250 μ F/250V ($R_s=44m\Omega$)
Output capacitor (C_o)	250 μ F/250V ($R_s=44m\Omega$)
Power diodes (V_{D1}, V_{D2})	1N4148-11A

A. SIMULATION RESULTS OF VARIOUS OUTPUT

1) simulation output of input dc voltage

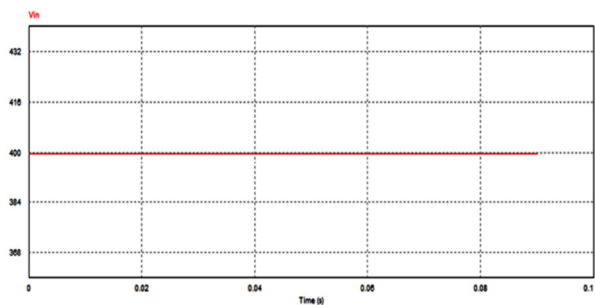


Figure 4.2(a).Waveform of input voltage

In this figure shows the input voltage of 400V dc supply for the proposed system.

2) simulation output of output dc voltage

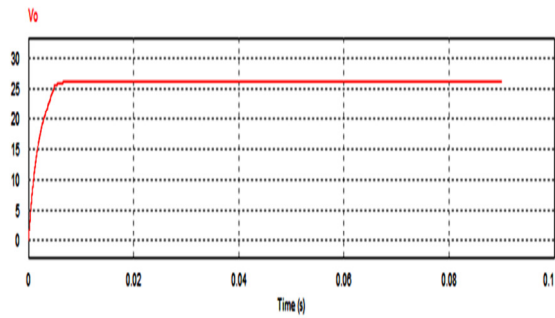


Figure 4.2(b) .Waveform of output DC voltage

This figure shows the constant DC voltage output of 25 volt for the proposed system.

3) simulation output of voltage stresses of v_{d1} voltage

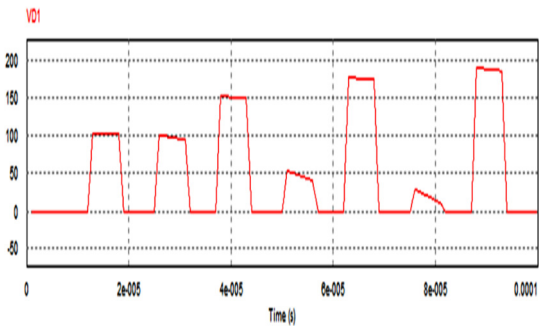


Figure 4.2(c).Waveform of voltage stresses of V_{D1} voltage

4) simulation output of inductor current i_{L1}

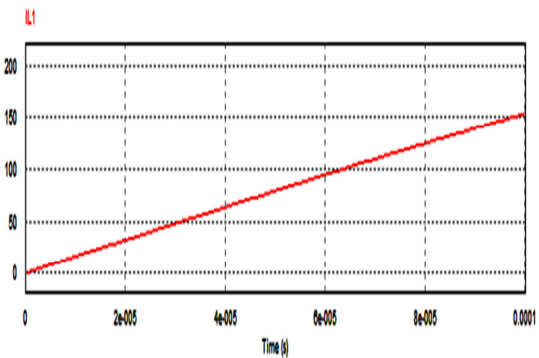


Figure 4.2(d).Waveform of inductor current I_{L1}

5) simulation output of inductor current i_{L2}

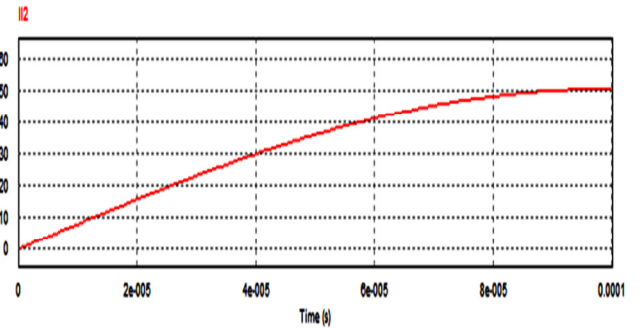


Figure .4.2(e) Waveform of inductor current I_{L2}

B. CONVERSION RATIO FOR VARIOUS DUTY CYCLE

As duty cycle increases the conversion ratio also increases and the output voltage is increases.

Thus the conversion ratio M is calculated by

$$M = \frac{V_o}{4} = \frac{D}{4}$$

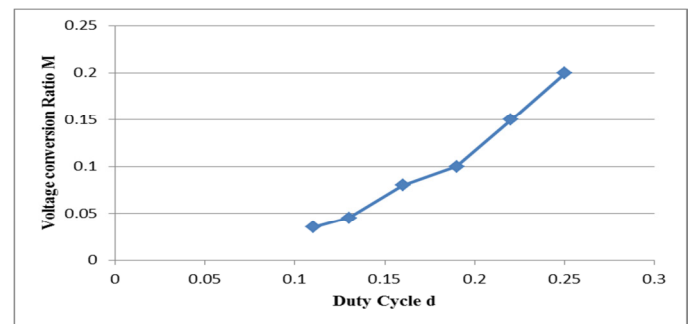


Figure 4.3 Conversion ratio for various duty cycle

C. MEASURED EFFICIENCY FOR VARIOUS INPUT VOLTAGE

Efficiency of the converter is calculated by

$$\eta = \frac{P_{OUT}}{P_{IN}} \times 100$$

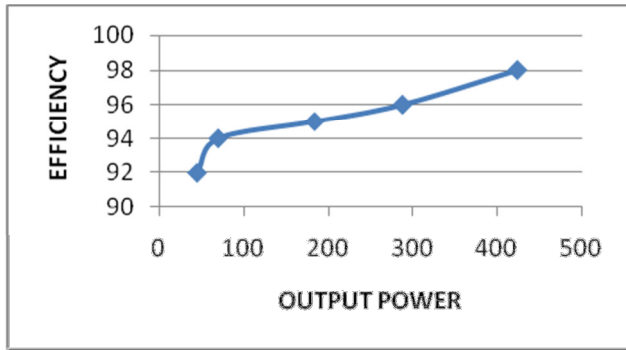


Figure 4.4 Efficiency curve for various input voltage

The above graph shows the efficiency for various input voltages. As input voltage increases the input power and also the output power increases. Due to that the efficiency of the converter is increased.

V. CONCLUSION

Thus the proposed, a novel transformerless interleaved high step-down conversion ratio dc-dc converter with low switch voltage stress has been simulated and results are obtained. In this project, two input capacitors are series-charged by the input voltage and parallel discharged by a new two-phase IBC for providing a much higher step-down conversion ratio without adopting an extreme short duty cycle. Based on the capacitive voltage division, the main objectives of the new voltage-divider circuit in the converter are both storing energy in the blocking capacitors for increasing the step-down conversion ratio and reducing voltage stresses of active switches. It will allow to choose lower voltage rating MOSFETs to reduce both switching and conduction losses, and the overall efficiency is consequently improved. This is very suitable for applications requiring high step-down conversion ratio.

VI. REFERENCES

1. D.-C. Lu and V. G. Agelidis, "Photovoltaic-battery-powered dc bus system for common portable electronic devices," *IEEE Trans. Power Electron.*, vol. 24, no. 3, pp. 849–855, Mar. 2009.
2. K. Sun, L. Zhang, Y. Xing, and J. M. Guerrero, "A distributed control strategy based on dc bus signaling for modular photovoltaic generation systems with battery energy storage," *IEEE Trans. Ind. Electron.*, vol. 26, no. 10, pp. 3032–3045, Oct. 2010.
3. H. R. E. Larico and I. Barbi, "Three-phase push-pull dc-dc converter: Analysis, design, experimentation," *IEEE Trans. Ind. Electron.*, vol. 59, no. 12, pp. 4629–4636, Dec. 2012.
4. Garcia, P. Zumel, A. D. Castro, and J. A. Cobos, "Automotive dc-dc bidirectional converter made with many interleaved buck stages," *IEEE Trans. Power Electron.*, vol. 21, no. 3, pp. 578–586, May 2006.
5. J. P. Rodrigues, S. A. Mussa, M. L. Heldwein, and A. J. Perin, "Three level ZVS active clamping PWM for the dc-dc buck converter," *IEEE Trans. Power Electron.*, vol. 24, no. 10, pp. 2249–2258, Oct. 2009.
6. Y. M. Chen, S. Y. Teseng, C. T. Tsai, and T. F. Wu, "Interleaved buck converters with a single-capacitor turn-off snubber," *IEEE Trans. Aerosp. Electron. Syst.*, vol. 40, no. 3, pp. 954–967, Jul. 2004.
7. T. Tsai and C. L. Shen, "Interleaved soft-switching coupled-buck converter with active-clamp circuits," in *Proc. IEEE Int. Conf. Power Electron. Drive Syst.*, 2009, pp. 1113–1118.
8. K. Yao, Y. Qiu, M. Xu, and F. C. Lee, "A novel winding-coupled buck converter for high-frequency, high-step-down dc-dc conversion," *IEEE Trans. Power Electron.*, vol. 20, no. 5, pp. 1017–1023, Sep. 2005.
9. K. Yao, M. Ye, M. Xu, and F. C. Lee, "Tapped-inductor buck converter for high-step-down dc-dc conversion," *IEEE Trans. Power Electron.*, vol. 20, no. 4, pp. 775–780, Jul. 2005.
10. I.-O. Lee, S.-Y. Cho, and G.-W. Moon, "Interleaved buck converter having low switching losses and improved step-down conversion ratio," *IEEE Trans. Power Electron.*, vol. 27, no. 8, pp. 3664–3675, Aug. 2012.
11. L. Sung-Sae, "Step-down converter with efficient ZVS operation with load variation," *IEEE Trans. Ind. Electron.*, vol. 61, no. 1, pp. 591–597.